ISSN: 1410-8917
Jurnal Kimia Sains & Aplikasi
e-ISSN: 2597-9914

Jurnal Kimia Sains dan Aplikasi 27 (6) (2024): 265-270

Jurnal Kimia Sains dan Aplikasi
Journal of Scientific and Applied Chemistry

Journal homepage: http://ejournal.undip.ac.id/index.php/ksa

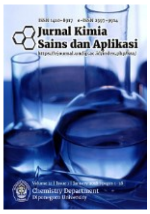

Effect of Precursors Concentration on The Optical and Photoelectrochemical Properties of Bi_2S_3/TiO_2 Nanotubes Arrays Photoanode Synthesized by the SILAR Technique

Eko Martin Sinaga [1,*], Muhammad Iqbal Syauqi [1], Jarnuzi Gunlazuardi [1]

[1] Department of Chemistry, Faculty of Mathematics and Natural Sciences, University of Indonesia, Depok, 16424, Indonesia

* Corresponding author: ekomartinsinaga972@gmail.com

https://doi.org/10.14710/jksa.27.6.265-270

Article Info

Article history:

Received: 13th January 2024
Revised: 08th May 2024
Accepted: 28th May 2024
Online: 30th June 2024

Keywords:
Bi_2S_3; Precursor concentration; SILAR; TiO_2 NTAs

Abstract

The use of robust solar energy-driven photocatalysis materials to address the global energy and environmental crisis has gained significant attention in recent years. However, the wide band gaps in many robust semiconductor photocatalysts hinder their absorption of visible light from the solar spectrum. To address this issue, the modification of the large band gap semiconductor with the lower band gap material using the Successive Ionic Layers Adsorption and Reaction (SILAR) technique has emerged as an economical, accessible, and reproducible method for depositing nanoscale materials onto semiconductor substrates. This research aims to know how the concentration variation of cation and anion precursors in the SILAR technique affects the optical and photoelectrochemical properties of the resulting composite materials. Bi_2S_3 serves as a modifier for TiO_2 nanotube arrays (NTAs). The result shows that the cation-anion concentration ratio of 1:1.5 mM with five SILAR cycles gives the best photoelectrochemical performance, with a stable current density of 0.12 mA/cm^2, compared to pristine TiO_2 NTAs the current density of Bi_2S_3/TiO_2 NTAs is 15-fold. In addition, at each variation, the concentration ratio of cation and anion precursors decreases bandgap energy with each increase in the SILAR cycle.

1. Introduction

The world is dealing with enormous challenges related to energy security and environmental sustainability [1]. The use of fossil fuels contributes to environmental pollution by releasing carbon dioxide into the atmosphere, and the continuing depletion of fossil fuels seriously threatens the global community [2]. In addition, the increasing amount of hazardous industrial waste being disposed of raises serious environmental concerns with industry advancement. As a result, efforts are being undertaken to investigate technology for enhanced ecological cleanup and renewable energy sources [3]. It requires material that supports the objectives of obtaining renewable energy sources and environmental restoration.

Several semiconductor photocatalysts, such as WO_3, TiO_2, CdS, Bi_3NbO_7, ZnO, Cu_2O, CdO, SnO_2, Al_2O_3, SiO_2, Fe_2O_3, have been used recently for various photocatalytic applications due to their potential chemical and physical properties, as well as their improved chemical stability and stable electronic structure. Among them, TiO_2 is an intriguing material due to its distinct oxide characteristics [4, 5]. Three crystal forms of titanium (IV) dioxide exist, e.g., rutile, which is thermodynamically stable, anatase, and metastable brookite. In those forms, Ti^{4+} coordinates with six oxygen atoms (O^{2-}) [6].

Notably, TiO_2 in nanotube arrays (NTAs) especially attracts interest due to its porous, one-dimensional structure, offering a higher specific surface area and improved electron-hole transfer efficiency [7]. However, despite these advantages, pristine TiO_2 NTAs exhibit limited photocatalytic activity outside the UV region due to their wide band gap (3.0–3.2 eV). To overcome this limitation, various modification strategies such as doping, dye sensitization, and junction formation with lower band gap materials are commonly employed.

Bi_2S_3 semiconductor is a significant semiconductor within the V-VI family of materials, drawing technological interest due to recent research advancements. It finds potential applications in various fields, such as supercapacitors, photocatalysis, and fluorescent markers [8]. As an orthorhombic n-type semiconductor with a band gap of ~1.7 eV, Bi_2S_3 efficiently absorbs visible light in the range of 400 to 900 nm [9]. Sensitizing TiO_2 NTAs with Bi_2S_3 enhances the photocatalytic activity compared to their pristine counterparts due to the matched band potentials [10, 11]. Furthermore, the low cost, natural abundance, non-toxicity, and environmental friendliness of Bi_2S_3 further enhance its applicability [12, 13].

Successive Ionic Layers Adsorption and Reaction (SILAR) is a method that can be employed to fabricate TiO_2 NTAs sensitized with Bi_2S_3 material. SILAR is known for its straightforward process, cost-effectiveness, and shorter deposition time, making it advantageous for depositing thin films of binary semiconductors [12]. Using the SILAR approach, weakly bound species are eliminated by immersing the substrate separately in two precursor solutions and then washing it between them with the appropriate solvent, allowing the formation of the well-dispersed nanomaterials on the substrate [14]. Therefore, a SILAR cycle entails the following steps, i.e., adsorption of cation precursors, solvent flushing, adsorption of anion precursors, further reactions, and rinsing [15]. Concisely, the SILAR approach prevents homogenous precipitation in the solution by successive flushing with the appropriate solvent between each immersion and utilizing the precursor solution's adsorption and ion reaction [16, 17].

The synthesis of Bi_2S_3/TiO_2 NTAs material reported previously was mainly conducted at a fixed concentration [12, 14]. However, it is recognized that the concentration of precursors significantly influences the character of the resulting precipitate in the SILAR method [17]. Therefore, this study proposes a different set of cation and anion concentrations for the SILAR synthesis process. Specifically, we investigate how varying concentrations affect the optical and photoelectrochemical properties of Bi_2S_3/TiO_2 NTAs. The concentration ratios used in this research were varied as follows: 1 mM: 1.5 mM, 2 mM: 3 mM, and 10 mM: 30 mM.

2. Experimental

2.1. Materials

The materials used in this research were titanium plate (99.6% purity), acetone (C_3H_6O), ethanol (C_2H_5OH), ammonium fluoride (NH_4F), ethylene glycol ($C_2H_6O_2$), bismuth nitrate pentahydrate ($Bi(NO_3)_3.5H_2O$), sodium sulfide trihydrate ($Na_2S.3H_2O$), sodium sulfate (Na_2SO_4), mannitol ($C_6H_{14}O_6$), deionized water was purchased commercially. All materials were obtained from Sigma-Aldrich, except for the titanium plate obtained from Baoji Jinsheng Metal Material Co., Ltd. and deionized water from OneMed.

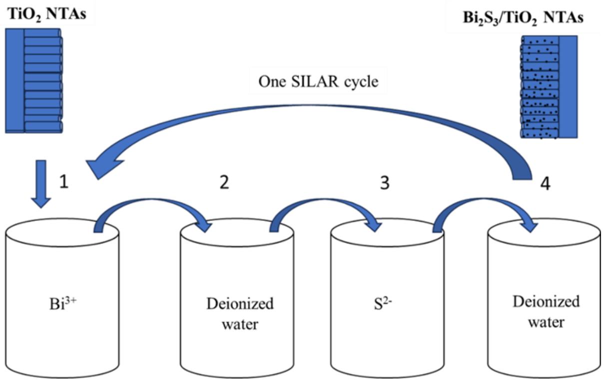

Figure 1. Successive Ionic Layers Adsorption and Reaction (SILAR) illustration on the synthesis of Bi_2S_3 deposited on the TiO_2 nanotubes array

2.2. Synthesis of TiO_2 NTAs

Titanium foil with a 0.2 mm thickness was cleaned by sonicating it at room temperature for 15 minutes in C_2H_5OH and C_3H_6O solutions, after which it was rinsed with distilled water and left to air dry. Every anodization experiment was conducted using a two-electrode electrochemical cell. Pt was utilized as the cathode, and the Ti plate (6 × 1.5 × 0.02 cm) was used as the anode. An electrolyte consisting of 2% H_2O and 0.3% NH_4F was a $C_2H_6O_2$ solution. The two electrodes were spaced apart by about 1.5 centimeters. At a potential of 50 V, the anodization process was run for 60 minutes. Following the anodization procedure, the sample was immersed and dried, then calcined for 2 hours at a temperature of 450°C with a temperature rise rate of 5°C/min [18].

2.3. Synthesis of Bi_2S_3/TiO_2 Nanotubes Arrays (Bi_2S_3/TiO_2 NTAs) by SILAR Method

Bi_2S_3 on the surface of TiO_2 NTAs was synthesized using the SILAR method with variations of SILAR cycles 1, 3, 5, and 7, as illustrated in Figure 1. In addition, this research was also compared to variations of concentrations for precursor cations and anions. The concentration variation (mM) used were 1: 1.5, 2: 3, and 10: 30. The proposed reaction mechanism for the formation of Bi_2S_3 is shown in Equations (1 to 3) [19].

$$2Bi^{3+} + 2C_8H_8(OH)_6 \rightarrow Bi_2(C_6H_8O_6) + C_6H_8(OH_2)_6^{6+} \quad (1)$$

$$Bi_2(C_6H_8O_6) + 3S^{2-} \rightarrow Bi_2S_3 + C_6H_8O_6^{6-} \quad (2)$$

$$C_6H_8(OH_2)_6^{6+} + C_6H_8O_6^{6-} \rightarrow 2C_8H_8(OH)_6 \quad (3)$$

2.4. Characterization of Materials

TiO_2 NTAs and Bi_2S_3/TiO_2 NTAs were characterized using FTIR (SHIMADZU IR Prestige-21), UV-Vis diffuse reflectance spectroscopy (UV-Vis DRS) (Shimadzu UV-2450), and Potentiostat. Meanwhile, the band gap energy value was determined using the UV-Vis DRS employing the Kubelka-Munk and Tauc plot method, according to Equation (4) [20].

$$(\alpha h v)^{\frac{1}{n}} = A\,(hv - Eg) \quad (4)$$

$$F(R) = \frac{(1-R)^2}{2R} \quad (5)$$

where R is the diffuse reflectance value, h is Plank's constant, n is the frequency of vibration, α is the absorption coefficient, Eg is the band gap, A is the proportional constant, and n depends on the band structure of the sample is 2 for indirect allowed transition (n = 2), due to TiO_2 in amorphous and anatase phase exhibiting indirect electron transfer [21].

$$(F(R)h\nu)^{1/2} = A\,(h\nu - Eg) \quad (6)$$

The F(R) values were plotted versus energy photon values according to the Tauc plot, where the Eg was determined at the F(R) value equal to zero.

In this research report, the morphology of the resulting material is not presented. However, based on the anodization and SILAR techniques employed, previous studies have confirmed that TiO_2 NTAs possess a diameter of 67.91 nm and a height of 4.4 µm [16].

2.5. Measurement of Photoelectrochemical Performance (PEC)

The preparation of photoelectrochemical cells was carried out using a potentiostats 3-electrode system. Working electrodes were TiO_2 NTAs and Bi_2S_3/TiO_2 NTAs. Meanwhile, the counter electrode was Pt, and the reference electrode was Ag/AgCl. A 40-watt Philips tungsten lamp was used as a visible light source. TiO_2 NTAs and Bi_2S_3/TiO_2 NTAs were tested utilizing 0.1 M Na_2SO_4 electrolyte. The test was carried out using the Multi Pulse Amperometry (MPA) in dark and light conditions for 10 seconds each other, and the applied potential was set at 0 V.

3. Results and Discussion

3.1. UV-Vis DRS Characterization of TiO_2 Nanotube Arrays

The anodization of titanium metal plate in $C_2H_6O_2$ containing water and fluoride ions produces an immobilized thick film of a highly ordered titanium oxide (TiO_2 NTAs). The results of UV-Vis DRS characterizations are presented in Figure 2a and Figure 2b. The TiO_2 NTAs show a typical reflectance spectrum in the 200-800 nm wavelength range [22]. The step decrease in %R occurs at wavelengths under 400 nm, which indicates that the absorption area of TiO_2 NTAs is in the UV region. It is important to note that the low %R values observed at wavelengths between 500 and 800 nm are attributed to refractive phenomena rather than absorption, as previously reported [23]. Based on this spectrum, the Kubelka-Munk and Tauc equations were used to create the Tauc plot, and the band gap was determined to be 3.2 eV.

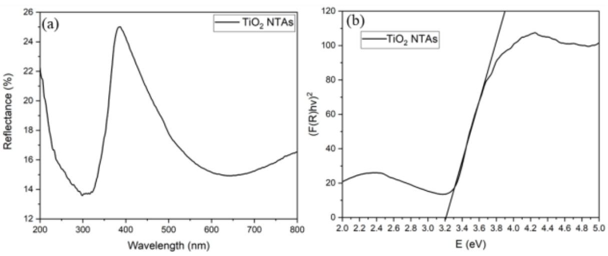

Figure 2. (a) UV-Vis DRS spectra of TiO_2 NTAs, (b) The absorption spectra of the corresponding sample by plotting $(F(R)h\nu)^2$ vs. E

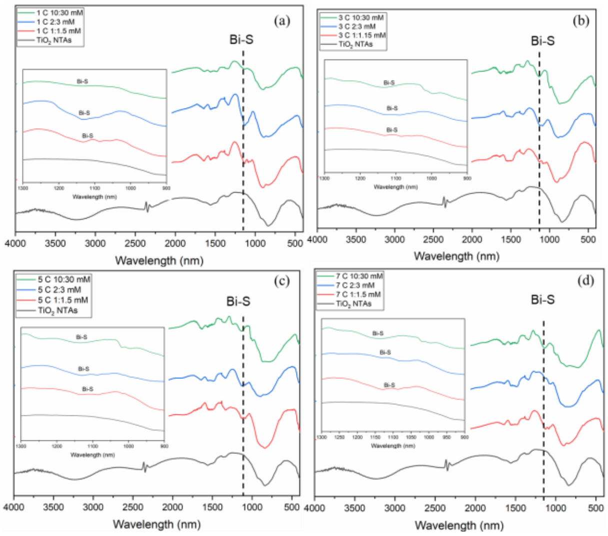

Figure 3. FTIR spectra of heterostructure Bi_2S_3/TiO_2 NTAs with variation concentration precursor cation and anion comparing with TiO_2 NTAs (a) 1-cycle SILAR, (b) 3-cycle SILAR, (c) 5-cycle SILAR, (d) 7-cycle SILAR

3.2. Synthesis of Bi_2S_3/TiO_2 NTAs

The synthesized Bi_2S_3/TiO_2 NTAs by the SILAR approach were used to deposit Bi_2S_3 nanoparticles onto the surface of TiO_2 NTAs (Figure 1). The following protocols were put into place, i.e., separately dissolves of $Bi(NO_3)_3$ in 50 milliliters 0.1 M mannitol solution (solution A) and $Na_2S.3H_2O$ in 50 milliliters of deionized water (solution B). Firstly, TiO_2 NTAs were soaked in solution A for three minutes, rinsed with deionized water, and then dipped in solution B for three minutes before being rinsed with deionized water. For the first cycle, it was sufficient to precipitate Bi_2S_3 particles on TiO_2 NTAs. The process was repeated several times to increase the loading of Bi_2S_3. The samples were labeled 1, 3, 5, and 7 cycles to distinguish them from one another. The thin films produced were dried at 60°C for an hour [24].

3.3. FTIR Characterization of Bi_2S_3/TiO_2 NTAs

The FTIR spectra in Figure 3 confirmed the presence of the conventional Bi-S-Bi vibration at wavenumber ~1100-1200 cm^{-1} and SH group stretching, which is visible at wavenumber 1344 cm^{-1}, indicating the successful of Bi_2S_3 deposition onto TiO_2 NTAs [16]. In addition, the absorption of functional groups by OH bending and OH stretching are also observed at wavenumbers 1540 cm^{-1} and 3247 cm^{-1} [19]. It also observed that the absorption of Bi-S at ~1130 cm^{-1} increases with the number of cycles and the concentration ratio, while shifting to a larger wavenumber. This indicates that the deposition of Bi_2S_3 onto TiO_2 NTAs was successful.

3.4. Optical Band Gap of Bi_2S_3/TiO_2 NTAs

Figure 4 (a, b, and c) displays the Tauc Plot of TiO_2 NTAs and Bi_2S_3/TiO_2 NTAs of each concentration variation, while the band gap calculation summary of every sample is presented in Figure 4d. The results confirm that the addition of Bi_2S_3 at varying concentrations reduces the band gap of TiO_2 NTAs. An increase in SILAR cycles further decreases the band gap values, indicating that more Bi_2S_3 is deposited with additional cycles. As the concentration of precursors increases, the band gap reduction in each cycle becomes more pronounced, signifying higher Bi_2S_3 deposition in more concentrated precursors. This is characterized by the absorption shift to the visible region and the corresponding decrease in energy, resulting in a reduced band gap.

3.5. Photoelectrochemical Performance Using Multi Pulse Amperometry (MPA) Method Under Visible Light Irradiation

The performance of the prepared photoanode (Bi_2S_3/TiO_2 NTAs) in generating the electron-hole pair under a visible light source was evaluated by the MPA techniques. It can be observed that the photocurrent density remains a constant high value when the light is turned on and then quickly decreases to zero mA/cm² as long as the light is turned off, indicating that the photocurrent is generated due to the photoelectric conversion of the Bi_2S_3/TiO_2 NTAs photoelectrode, and the electron transport rate is very fast. In addition, spikes in all Bi_2S_3/TiO_2 NTAs photoelectrodes can be observed when the light is intermittent, which is attributed to the accumulation of charge carriers.

Figure 5 shows a considerable photocurrent density that evolved when the visible light was switched ON. The results of this measurement showed the maximum electrochemical performance for each change in concentration and the cycles that vary with variation. The optimum electrochemical performance arises at 5 SILAR cycles (0.12 mA/cm²) for concentration variation of 1 mM: 1.5 mM (Figure 5a), the optimum electrochemical performance occurs at 3 SILAR cycles (0.05 mA/cm² and stable) for concentration ratio of 2 mM: 3 mM (Figure 5b), and the optimum electrochemical performance occurs at 1 SILAR cycle (0.14 Ma/cm² and unstable) for concentration ratio of 10 mM: 30 mM (Figure 5c).

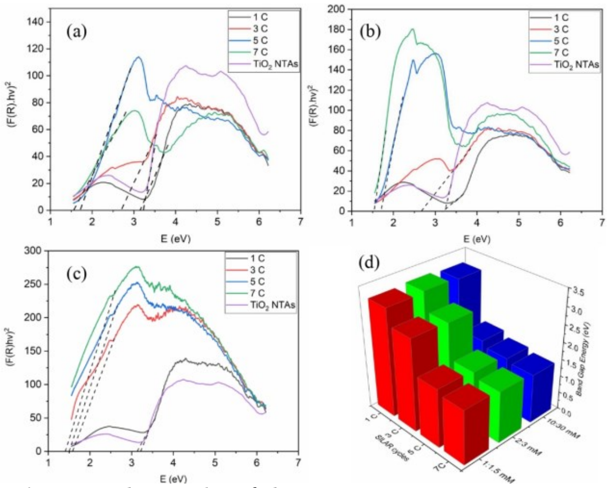

Figure 4. The results of characterization using UV-DRS for TiO_2 NTAs and Bi_2S_3/TiO_2 NTAs prepared by SILAR at different precursor concentrations and different cycles (a) Tauc plot for 1 mM of cationic and 1.5 mM of anionic, (b) Tauc plot for 2 mM of cationic and 3 mM of anionic, (c) Tauc plot for 10 mM of cationic and 30 mM of anionic, (d) diagram for summary band gap energy of Bi_2S_3/TiO_2 NTAs for different precursor concentrations and different cycles

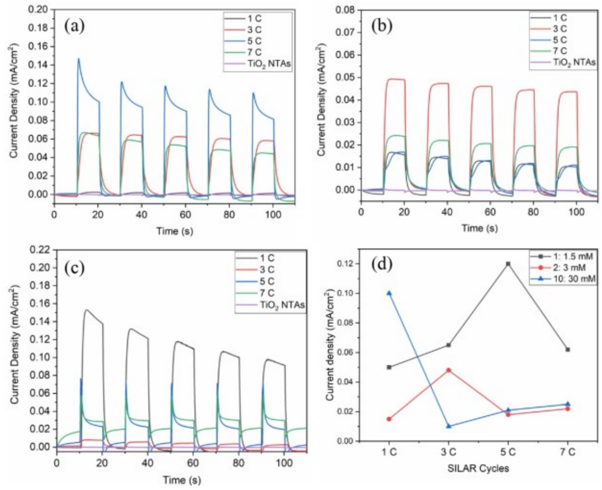

Figure 5. Photoelectrochemical performance of TiO_2 NTAs and Bi_2S_3/TiO_2 NTAs prepared by SILAR for different precursor concentrations and different cycles illuminated with visible light with (a) 1 mM of cationic and 1.5 mM of anionic, (b) 2 mM of cationic: 3 mM of anionic, (c) 10 mM of cationic: 30 mM of anionic, (d) summary of photoelectrochemical performance of Bi_2S_3/TiO_2 NTAs

Compared with the report conducted by Wang *et al.* [10], the best current density in 5 SILAR cycles with a ratio of cation and anion concentrations of 0.01 M: 0.01M using distilled water as a solvent. In addition, when compared to other research reports, maximum current density was obtained at 3 SILAR cycles with a ratio cation and anion concentrations of 0.01 M: 0.01 M. In that research report, the current density in 3 SILAR cycles is the maximum compared to other cycles; when compared to pure TiO_2 NTAs, the increase is fourfold [16]. In this research, the maximum current density is in 5 SILAR cycles for a ratio of 1 mM: 1.5 mM; when compared to pure TiO_2 NTAs, the increase is fifteenfold.

This is a consequence of the amount of Bi_2S_3 being deposited, which will also affect the material's surface. The photocurrent evolved due to the ability of Bi_2S_3 to absorb visible light to create exited and free electrons, which were subsequently injected into the TiO_2 NTAs conduction band and then produced photocurrent, which induced photocatalytic activity [25]. Based on PEC performance (MPA method), material TiO_2 NTAs before being deposited with Bi_2S_3 have a bad response to visible light compared with TiO_2 NTAs after being deposited with Bi_2S_3. It also confirmed the UV-DRS data of TiO_2 NTAs; the more bandgap energy of the TiO_2 shifts towards visible light, the more the current density increases. However, the resulting current density is also not maximized when it shifts to the visible area in optical properties.

4. Conclusion

This research applied the SILAR method to deposit Bi_2S_3 nanoparticles on TiO_2 NTAs as a photosensitizer as part of its evaluation. The results indicate that increasing the precursor concentration leads to greater deposition of Bi_2S_3, evidenced by a reduction in the band gap value. However, the over-deposited Bi_2S_3 impedes electron-hole mobility within the photoanode, consequently lowering the photocurrent performance. The best photoelectrochemical performance was shown by the Bi_2S_3/TiO_2 NTAs photoanode synthesized at a cation-anion ratio of 1 mM: 1.5 mM at 5 SILAR cycles with an energy band gap of 1.71 eV when compared to pristine TiO_2 has a fifteenfold increase in current density. For other ratios, the current density for a cation-to-anion concentration ratio of 2 mM: 3 mM at 3 SILAR cycles yields a steady-state photocurrent of ~0.01 mA cm^{-2}. Similarly, a concentration ratio of 10 mM: 30 mM at 1 SILAR cycle.

References

[1] Tanzim Ur Rahman, Hridoy Roy, Athkia Fariha, Afrina Zaman Shoronika, Md Rashid Al-Mamun, Syed Z. Islam, Md Shahinoor Islam, Hadi M. Marwani, Aminul Islam, Abdulmohsen K. D. Alsukaibi, Mohammed M. Rahman, Md Rabiul Awual, Progress in plasma doping semiconductor photocatalysts for efficient pollutant remediation and hydrogen generation, *Separation and Purification Technology*, 320, (2023), 124141 https://doi.org/10.1016/j.seppur.2023.124141

[2] Ghaferah H. Al-Hazmi, Moamen S. Refat, Khaled F. Alshammari, Khadiza Tul Kubra, Ahmed Shahat, Efficient toxic doxorubicin hydrochloride removal from aqueous solutions using facial alumina nanorods, *Journal of Molecular Structure*, 1272, (2023), 134187 https://doi.org/10.1016/j.molstruc.2022.134187

[3] Md Shad Salman, Md Chanmiya Sheikh, Md Munjur Hasan, Md Nazmul Hasan, Khadiza Tul Kubra, Ariyan Islam Rehan, Mrs Eti Awual, Adiba Islam Rasee, R. M. Waliullah, Mohammed Sohrab Hossain, Md Abdul Khaleque, Abdulmohsen K. D. Alsukaibi, Hamed M. Alshammari, Md Rabiul Awual, Chitosan-coated cotton fiber composite for efficient toxic dye encapsulation from aqueous media, *Applied Surface Science*, 622, (2023), 157008 https://doi.org/10.1016/j.apsusc.2023.157008

[4] Ankit Kumar Vishwakarma, Ajaya Kumar Sharma, Ashok Kumar Mishra, Lallan Yadava, A titanium dioxide-based thick film gas sensor for propanol, *Materials Letters: X*, 17, (2023), 100184 https://doi.org/10.1016/j.mlblux.2023.100184

[5] Sry Wahyuni, Syukri Syukri, Syukri Arief, Green synthesis of Ag/TiO_2 Nanocomposite Assisted by Gambier Leaf (*Uncaria gambir* Roxb) Extract, *Jurnal Kimia Sains dan Aplikasi*, 22, 6, (2019), 250-255 https://doi.org/10.14710/jksa.22.6.250-255

[6] Wanbiao Hu, Liping Li, Guangshe Li, Yun Liu, Ray L. Withers, Atomic-scale control of TiO_6 octahedra through solution chemistry towards giant dielectric response, *Scientific Reports*, 4, (2014), 6582 https://doi.org/10.1038/srep06582

[7] Sherly Kasuma Warda Ningsih, Muhammad Iqbal Syauqi, Rahmat Wibowo, Jarnuzi Gunlazuardi, Effect of potential variation on morphology and photoelectrochemical properties of TiO_2 nanotube arrays (TNAs) by two-step anodization method, *Journal of Applied Electrochemistry*, 54, 4, (2024), 739-756 https://doi.org/10.1007/s10800-023-01999-5

[8] I. A. T. Gaia, E. V. Guimarães, P. I. S. Maia, H. D. Mikhail, M. S. da Luz, A. C. A. S, R. S. Silva, Synthesis and investigation of optical and structural properties of Bi_2O_3/Bi_2S_3 nanoparticles in an aqueous solution, *Physica B: Condensed Matter*, 662, (2023), 414947 https://doi.org/10.1016/j.physb.2023.414947

[9] Minghua Wang, Longyu Yang, Jinyun Yuan, Linghao He, Yingpan Song, Hongzhong Zhang, Zhihong Zhang, Shaoming Fang, Heterostructured $Bi_2S_3@NH_2$-MIL-125(Ti) nanocomposite as a bifunctional photocatalyst for Cr(VI) reduction and rhodamine B degradation under visible light, *RSC Advances*, 8, 22, (2018), 12459-12470 https://doi.org/10.1039/C8RA00882E

[10] Qingyao Wang, Zhiyuan Liu, Rencheng Jin, Ying Wang, Shanmin Gao, SILAR preparation of Bi_2S_3 nanoparticles sensitized TiO_2 nanotube arrays for efficient solar cells and photocatalysts, *Separation and Purification Technology*, 210, (2019), 798-803 https://doi.org/10.1016/j.seppur.2018.08.050

[11] Abrar Ahmad, Fatih Tezcan, Gurbet Yerlikaya, Rehman Zia ur, Halime Paksoy, Gülfeza Kardaş, Three dimensional rosette-rod TiO_2/Bi_2S_3 heterojunction for enhanced photoelectrochemical water splitting, *Journal of Alloys and Compounds*, 868, (2021), 159133 https://doi.org/10.1016/j.jallcom.2021.159133

[12] P. Sreedev, V. Rakhesh, N. S. Roshima, Balakrishnan Shankar, Preparation of Zinc Oxide Thin films by SILAR method and its Optical analysis, *Journal of Physics: Conference Series*, 1172, (2019), 012024 https://doi.org/10.1088/1742-6596/1172/1/012024

[13] Xinli Li, Xueyang Han, Di Zhu, Yongchao Chen, Lihua Li, Zhanhong Ma, Yongjun Gu, Fengzhang Ren, Jinliang Huang, Improvement of photoelectric properties of TiO_2/Bi_2S_3 composite film by annealing treatment, *Optical Materials*, 91, (2019), 101-107 https://doi.org/10.1016/j.optmat.2019.03.015

[14] B. R. Sankapal, R. S. Mane, C. D. Lokhande, Successive ionic layer adsorption and reaction (SILAR) method for the deposition of large area (~10 cm^2) tin disulfide (SnS_2) thin films, *Materials Research Bulletin*, 35, 12, (2000), 2027-2035 https://doi.org/10.1016/S0025-5408(00)00405-0

[15] Ines Khemissi, Lotfi Khezami, Khaled Trabelsi, Ahlem Guesmi, Abdessalem Kouki, John Kiwi, Brahim Bessais, Sami Rtimi, Anouar Hajjaji, Stable Ta_2O_5 nanotubes decorated by PbS by the SILAR method for photocatalytic dye degradation, *Journal of Photochemistry and Photobiology A: Chemistry*, 444, (2023), 114937 https://doi.org/10.1016/j.jphotochem.2023.114937

[16] Hawraa Sabah Hreo, Araa Mebdir Holi, Asla Abdullah Al-Zahrani, Asmaa Kadim Ayal, M. R. Almamari, Highly crystalline anatase TiO_2 nanotubes array films enhanced with Bi_2S_3 for photoelectrochemical applications, *Bulletin of Materials Science*, 45, 4, (2022), 205 https://doi.org/10.1007/s12034-022-02781-7

[17] Samantha Prabath Ratnayake, Jiawen Ren, Elena Colusso, Massimo Guglielmi, Alessandro Martucci, Enrico Della Gaspera, SILAR Deposition of Metal Oxide Nanostructured Films, *Small*, 17, 49, (2021), 2101666 https://doi.org/10.1002/smll.202101666

[18] F. K. An'nur, B. V. Wihelmina, J. Gunlazuardi, R. Wibowo, Tandem system of dyes sensitized solar cell–photo electro chemical (DSSC-PEC) employing TiO_2 nanotube/BiOBr as dark cathode for nitrogen

fixation, *AIP Conference Proceedings*, 2243, (2020), 020002 https://doi.org/10.1063/5.0001100

[19] Prita Amelia, Jarnuzi Gunlazuardi, Development of $BiOBr/TiO_2$ nanotubes electrode for conversion of nitrogen to ammonia in a tandem photoelectrochemical cell under visible light, *International Journal of Renewable Energy Development*, 12, 4, (2023), 702-710 https://doi.org/10.14710/ijred.2023.51314

[20] Teressa Binte Mohsin, S. M. Abidul Islam, Tahmina Tabassum Tonni, M. M. Rhaman, Analysis of conductivity and band-gap energy of bismuth ferrite nanoparticles as prospective photovoltaic material, *Materials Today: Proceedings*, (2023), https://doi.org/10.1016/j.matpr.2023.01.330

[21] Naeimeh Sadat Peighambardoust, Shahin Khameneh Asl, Raheleh Mohammadpour, Shahab Khameneh Asl, Band-gap narrowing and electrochemical properties in N-doped and reduced anodic TiO_2 nanotube arrays, *Electrochimica Acta*, 270, (2018), 245-255 https://doi.org/10.1016/j.electacta.2018.03.091

[22] Mahnaz Darrudi, Hossein Tavakol, Mohamad Mohsen Momeni, Electrochemical co-deposition of cobalt and graphene, produced from recycled polypropylene, on TiO_2 nanotube as a new catalyst for photoelectrochemical water splitting, *International Journal of Hydrogen Energy*, 48, 9, (2023), 3495-3510 https://doi.org/10.1016/j.ijhydene.2022.10.145

[23] T. Raguram, K. S. Rajni, Synthesis and characterisation of Cu - Doped TiO_2 nanoparticles for DSSC and photocatalytic applications, *International Journal of Hydrogen Energy*, 47, 7, (2022), 4674-4689 https://doi.org/10.1016/j.ijhydene.2021.11.113

[24] Zhi Wu, Ding Yuan, Sheng Lin, Wenxi Guo, Dongping Zhan, Lan Sun, Changjian Lin, Enhanced photoelectrocatalytic activity of $Bi_2S_3–TiO_2$ nanotube arrays hetero-structure under visible light irradiation, *International Journal of Hydrogen Energy*, 45, 56, (2020), 32012-32021 https://doi.org/10.1016/j.ijhydene.2020.08.258

[25] J. L. Qiao, Q. Y. Wang, J. X. Ye, Y. K. Xiao, Enhancing photoelectrochemical performance of TiO_2 nanotube arrays by CdS and Bi_2S_3 co-sensitization, *Journal of Photochemistry and Photobiology A: Chemistry*, 319-320, (2016), 34-39 https://doi.org/10.1016/j.jphotochem.2015.12.020